ISSN 1070-3284, Russian Journal of Coordination Chemistry, 2014, Vol. 40, No. 10, pp. 773–780. © Pleiades Publishing, Ltd., 2014.

pH-Dependent Synthesis of Two New Lead(II) Coordination Polymers with 4-Aminoantipyrine and 5-Nitroisophthalate Ligands[1]

Q. Wang, L. C. Kong, Y. Wang, E. C. Yang*, and X. J. Zhao**

College of Chemistry, Tianjin Key Laboratory of Structure and Performance for Functional Molecules, Key Laboratory of Inorganic-Organic Hybrid Functional Material Chemistry, Ministry of Education, Tianjin Normal University, Tianjin, 300387 P.R. China

**e-mail: encui_yang@163.com; **xiaojun_zhao15@163.com*

Received April 29, 2014

Abstract—Two novel lead(II) coordination polymers with the same mixed ligands, $[Pb(AAP)(NIP)]_n$ (**I**) and $\{[Pb(AAP)(NIP)] \cdot 2H_2O\}_n$ (**II**) (AAP = 4-aminoantipyrine and NIP^{2-} = 5-nitroisophthalate), were prepared by controlling the pH value of the reaction mixture. Complexes **I** and **II** were characterized by X-ray single-crystal diffraction analyses (CIF files CCDC nos. 936101 (**I**) and 936102 (**II**)). Complex I with terminal AAP molecule displays a linear chain with hemidirected Pb^{2+} ions connected by *bis*-bidentate chelating-NIP^{2-} anions. By contrast, complex **II** exhibits a dimeric $\{Pb_2(AAP)_2\}$-based coplanar layer extended by bidentate chelating-bidentate chelating and bridging-NIP^{2-} anions. Obviously, the pH-directed structural difference is dominated by the competitive binding modes of the AAP and carboxylate groups of NIP^{2-} ligands. Both complexes display different thermal stability due to structural difference and similar emissions originated from the intra- and/or inter-ligand electron transfer, suggesting their potential application as luminescent materials.

DOI: 10.1134/S1070328414100108

INTRODUCTION

Controllable design and synthesis of metal-organic frameworks (**MOFs**) with the same components and different structures have received a great deal of attention in coordination and supramolecular chemistry, owing to their intriguing structures, attractive topological features, as well as the promising applications in magnetism, gas sorption, and optical devices [1–3]. Apparently, the subtle manipulations of these self-assembly processes can be easily achieved by variously external factors, such as metal-ligand molar ratio [4], temperature and pressure [5–7], pH and type of the reactant medium [8, 9], template molecule [10] and counter anion [11–12]. Additionally, the choice of the reactant mixture, such as the single and/or mixed ligands and the metal ions with variable coordination polyhedra also becomes one of importantly intrinsic factors. The number, type, and spatial orientation of the binding group from the mixed ligand as well as the stereo and electronic preferences of the metal ion [13] can more significantly determine the overall structural diversity of the targeted complexes. Herein, as a continuation of the structural modification and property exploration on the luminescent MOFs [14], 4-aminoantipyrine (**AAP**) and 5-nitroisophthalic acid (**H_2NIP**) were selected as mixed ligands to self-assemble with inorganic Pb(II) source at different pH values. The special considerations for the investigation are that aromatic dicarboxylate ligand has pH-dependent multi-deprotonated forms, flexibly metallic bonding sites, and a large number of possibly cationic binding modes. AAP and its derivatives have popular bidentate N,O-chelating mode and are widely investigated in biological, analytical, clinical and optical device [15–17]. Acting as a heavy toxic metal with large radius, lead(II) is a favorable and fashionable building block with flexible coordination environment and various stereo-chemical activities, providing unique opportunities for the formation of unusual network topologies with interesting properties [18]. The combination of the two ligands with versatile Pb(II) ion can potentially generate interestingly functional MOFs. As a result, two luminescent coordination polymers with the formulas of $[Pb(AAP)(NIP)]_n$ (**I**) and $\{[Pb(AAP)(NIP)] \cdot 2H_2O\}_n$ (**II**) were obtained, exhibiting a linear chain with hemidirected Pb^{2+} ions connected by bis-bidentate chelating-NIP^{2-} ligands for **I** and a dimeric $\{Pb_2(AAP_2)\}$-based coplanar layer extended by bidentate chelating-bidentate chelating and bridging-NIP^{2-} anions for **II**. The structural difference of the two complexes is essentially dominated by the competitive coordination of carboxylate group and AAP ligand in different binding modes. Due to the presence of lattice water molecules, the two complexes display different thermal stability. Additionally, despite the structural difference, the both complexes give strong luminescent emissions resulting from the intra- and/or inter-ligand electron transfer.

[1] The article is published in the original.

EXPERIMENTAL

Reagents and instruments. All starting materials and solvents employed here were commercially available without further purification. Doubly deionized water was used for the conventional synthesis. Elemental analyses for C, H, and N were carried out with a PerkinElmer 2400C elemental analyzer. Fourier-transform (FT) IR spectra (KBr pellets) were taken on a Nicolet IR-200 spectrometer in the range 4000–400 cm^{-1}. Thermogravimetric analysis experiments were carried out on a Shimadzu simultaneous DTG-60A compositional analysis instrument from room temperature to 800°C under N_2 atmosphere at a heating rate of 10°C min^{-1}. Fluorescence spectra of the polycrystalline powder samples of **I** and **II** were performed on a Fluorolog-3 fluorescence spectrophotometer from Horiba Jobin Yvon at room temperature.

Synthesis of I. To a mixed methanol-water solution (v : v = 1 : 1, 10.0 mL) containing AAP (81.6 mg, 0.4 mmol) and H_2NIP (31.5 mg, 0.15 mmol) was slowly added an aqueous solution (5.0 mL) of $Pb(NO_3)_2$ (66.2 mg, 0.2 mmol) with constant stirring. The pH value of the mixture was adjusted to ~7.0 by triethylamine. The resulting mixture was further stirred for another one hour at room temperature and filtered. Yellow block-shaped crystals suitable for X-ray analysis were obtained by slow evaporation of the filtrate at room temperature in one week. The yield was 35% based on H_2NIP ligand.

For $C_{19}H_{16}N_4O_7Pb$			
anal. calcd., %:	C, 36.83;	H, 2.60;	N, 9.04.
Found, %:	C, 36.80;	H, 2.58;	N, 9.06.

IR (ν, cm^{-1}): 3468 ν(N–H), 3237 ν(N–H), 1619 $\nu_{as}(COO^-)$, 1521 $\nu_{as}(COO^-)$, 1451 $\nu_s(COO^-)$, 1359 $\nu_s(COO^-)$.

Synthesis of II. To a mixed methanol-water solution (v : v = 1 : 1, 10.0 mL) containing AAP (81.6 mg, 0.4 mmol) and H_2NIP (31.5 mg, 0.15 mmol) was slowly added an aqueous solution (5.0 mL) of $Pb(NO_3)_2$ (66.2 mg, 0.2 mmol) with constant stirring. The pH value of the mixture was adjusted to ~2.0 by an aqueous hydrochloric acid solution (0.1 mol L^{-1}). The resulting mixture was further stirred for another one hour at room temperature and filtered. Yellow block-shaped crystals suitable for X-ray analysis were obtained by slow evaporation of the filtrate at room temperature in one week. The yield was 30% based on H_2NIP.

For $C_{19}H_{20}N_4O_9Pb$			
anal. calcd., %:	C, 34.81;	H, 3.07;	N, 8.55.
Found, %:	C, 34.79;	H, 3.06;	N, 8.54.

IR (ν, cm^{-1}): 3411 ν_{br}(O–H), 3294 ν(N–H), 1622 $\nu_{as}(COO^-)$, 1530 $\nu_{as}(COO^-)$, 1448 $\nu_s(COO^-)$, 1356 $\nu_s(COO^-)$.

X-ray diffraction analysis. Single-crystal X-ray diffraction data for **I** and **II** were collected on a computer-controlled Bruker APEX-II CCD diffractometer equipped with graphite-monochromated MoK_α radiation with radiation wavelength 0.71073 Å by using ω-φ scan mode. Semiempirical multiscan absorption corrections were applied using SADABS [19] and the program SAINT [20] was used for integration of the diffraction profiles. Both structures were solved by direct methods and refined with the full-matrix least-squares technique using the SHELXS-97 and SHELXL-97 programs [21]. Anisotropic thermal parameters were assigned to all non-hydrogen atoms. The organic hydrogen atoms were generated geometrically. Details for crystallographic data were listed in Table 1, and selected bond lengths and angles were given in Table 2. Hydrogen-bonding parameters were shown in Table 3. Supplementary material has been deposited with the Cambridge Crystallographic Data Centre (nos. 936101 (**I**) and 936102 (**II**); deposit@ccdc.cam.ac.uk or http://www.ccdc.cam.ac.uk).

RESULTS AND DISCUSSION

Generated from the same reactant mixture, complexes **I** and **II** were successfully prepared with a molar ratio of 4 : 2 : 1.5 (AAP : Pb(II) : H_2NIP) by decreasing the pH value of the reactant mixture under ambient conditions. Notably, the neutral medium was adjusted by weak organic base and the low pH value was controlled by strong inorganic acid. In the IR spectra, a pair of weak absorptions between 3468 and 3237 cm^{-1} for **I** should be assigned to the stretching vibrations of N–H, indicating the presence of exocyclic amino group of AAP ligand. By contrast, a broad band centered at 3411 cm^{-1} and a weak band at 3294 cm^{-1} for **II** was corresponding to the characteristic vibrations of water molecule and amino moiety of AAP ligand. No obvious adsorption was observed at ~1700 cm^{-1}, confirming the complete deprotonation of the H_2NIP ligand. Additionally, the asymmetric (ν_{as}) and symmetric (ν_s) stretching vibrations of the deprotonated carboxylate group were located at 1619, 1521, 1451, and 1359 cm^{-1} for **I** and at 1622, 1530, 1448, and 1356 cm^{-1} for **II**. Their different separations ($\Delta\nu$ = 160 cm^{-1} for **I**, as well as 266 and 82 cm^{-1} for **II**) suggested the different coordination modes of the carboxylate group. Thus, the IR results were consistent with single-crystal structure analyses.

Single-crystal X–ray diffraction analyses show that complex **I**, $[Pb(AAP)(NIP)]_n$, features a linear one-dimensional (1D) chain with the unique Pb^{2+} ions linked by *bis*-bidentate chelating-NIP^{2-} anions, in which the terminal AAP molecules act as side arms to feature a comb-like motif. The asymmetric unit of **I**

Table 1. Crystallographic data and structure refinement summary for **I** and **II**

Parameter	Value	
	I	**II**
Formula weight	619.55	655.58
Crystal size, mm	0.15 × 0.14 × 0.13	0.16 × 0.13 × 0.11
Crystal system	Monoclinic	Triclinic
Space group	$C2/c$	$P\bar{1}$
a, Å	28.789(4)	8.2450(4)
b, Å	10.1143(16)	8.8995(4)
c, Å	13.769(2)	15.1208(7)
α, deg	90	91.163(1)
β, deg	102.857(3)	99.870(1)
γ, deg	90	107.297(1)
V, Å^3	3908.6(11)	1040.65(8)
Z	8	2
ρ_{calcd}, g/cm^3	2.106	2.092
μ_{Mo}, mm^{-1}	8.685	8.168
F(000)	2368	632
θ Range, deg	1.45–25.01	2.63–25.00
Range of reflection indices	$-34 \le h \le 25$, $-11 \le k \le 12$, $-16 \le l \le 16$	$-9 \le h \le 7$, $-10 \le k \le 10$, $-17 \le l \le 15$
Reflections collected/unique	9599/3441	5315/3634
R_{int}	0.0369	0.0183
Parameters	282	300
GOOF on F^2	1.003	1.063
$R(I > 2\sigma(I))$*	$R_1 = 0.0265$, $wR_2 = 0.0598$	$R_1 = 0.0273$, $wR_2 = 0.0697$
R (all reflections)*	0.0345/0.0637	0.0285/0.0707
$\Delta\rho_{max}/\Delta\rho_{min}$, e Å^{-3}	1.848/–1.330	2.822/–2.241

* $R_1 = \Sigma(\|F_o| - |F_c\|)$, $wR_2 = [\Sigma w(|F_o|^2 - |F_c|^2)^2/\Sigma w(F_o^2)^{]1/2}$.

contains one hexa-coordinated Pb^{2+} ion, one neutral AAP ligand, and one doubly deprotonated NIP^{2-} anion for charge compensation. As shown in Fig. 1a, the crystallographically independent Pb(II) site in **I** is in a NO_5 donor set provided by the exocyclic amino group and ketonic moiety from a bidentate N,O-chelating AAP molecule and two bidentate chelating carboxylate groups from two symmetry-related NIP^{2-} anions, displaying a hemidirected geometry. Obviously, the stereochemically active pair of electrons reside on the Pb^{2+} ion are above the basal plane. The bond lengths of Pb–O and Pb–N vary from 2.419(4) to 2.712(4) Å (Table 2), falling into the normal ranges [22–24].

Acting as an electronically neutral ligand, the AAP molecule adopts a bidentate N,O-chelating coordination mode to complete the metal coordination sphere. By contrast, two carboxylate groups of each NIP^{2-}

Table 2. Selected bond lengths (Å) and angles (deg) for **I*** and **II****

Bond	*d*, Å	Bond	*d*, Å
		I	
Pb(l)–N(3)	2.419(4)	Pb(l)–O(3)	2.484(2)
Pb(l)–O(5)^{i}	2.488(3)	Pb(l)–O(2)	2.601(4)
Pb(l)–O(1)	2.624(3)	Pb(l)–O(4)^{i}	2.712(4)
		II	
Pb(l)–N(3)	2.611(4)	Pb(l)–O(3)	2.476(3)
Pb(l)–O(5)^{i}	2.560(3)	Pb(l)–O(2)	2.679(3)
Pb(l)–O(2)^{ii}	2.742(3)	Pb(l)–O(4)^{i}	2.619(3)
Pb(l)–O(5)^{iii}	2.743(3)	Pb(l)–O(1)^{ii}	2.832(3)
Angle	ω, deg	Angle	ω, deg
		I	
N(3)Pb(l)O(3)	85.44(12)	N(3)Pb(l)O(5)^{i}	79.76(12)
O(3)Pb(l)O(5)	73.35(11)	N(3)Pb(l)O(2)	76.43(12)
O(3)Pb(l)O(2)	51.62(11)	O(5)^{i}Pb(l)O(2)	120/87(11)
N(3)Pb(l)O(l)	71.49(12)	O(3)Pb(l)O(l)	125.13(11)
O(5)^{i}Pb(1)O(1)	143.16(11)	O(2)Pb(l)O(l)	74.45(11)
N(3)Pb(l)O(4)^{i}	76.35(12)	O(3)Pb(l)O(4)^{i}	122.48(11)
O(5)^{i}(1)O(4)^{i}	50.05(10)	O(2)Pb(l)O(4)^{i}	152.57(12)
		II	
O(2)Pb(l)O(2)^{ii}	73.04(11)	O(3)Pb(l)N(3)	76.92(11)
O(5)^{i}Pb(1)O(5)^{iii}	75.23(11)	O(3)Pb(l)O(4)^{i}	123.99(10)
O(4)^{i}Pb(1)O(5)^{iii}	101.29(10)	N(3)Pb(l)O(4)^{i}	79.06(11)
O(2)^{ii}Pb(l)O(5)^{iii}	147.66(10)	O(5)^{i}Pb(l)O(2)	125.87(9)
O(3)Pb(l)O(2)	50.72(10)	O(4)^{i}Pb(l)O(2)	164.42(11)
N(3)Pb(l)O(2)	85.36(11)	O(5)^{i}Pb(1)O(2)^{ii}	136.84(10)
O(3)Pb(l)O(2)^{ii}	112.40(10)	O(4)^{i}Pb(1)O(2)^{ii}	99.68(10)
N(3)Pb(l)O(2)^{ii}	62.80(11)	O(3)Pb(l)O(5)^{iii}	74.83(10)
O(3)Pb(l)O(5)^{i}	75.22(10)	N(3)Pb(l)O(5)^{iii}	145.78(11)
O(5)^{i}Pb(l)N(3)	79.23(11)	O(2)Pb(l)O(5)^{iii}	91.42(9)
O(5)^{i}(1)O(4)^{i}	50.87(10)		

* Symmetry codes: ^{i} $x, y-1, z$ (**I**); ** ^{i} $x+1, y+1, z$; ^{ii} $1-x, 1-y, 1-z$; ^{iii} $1-x, -y, 1-z$ (**II**).

Table 3. Hydrogen bond lengths (Å) and bond angles (deg) for **I** and **II***

Contact D–H···A	Distance, Å			Angle
	D–H	H···A	D···A	D–H···A, deg
I				
N(3)–H(3*A*)···O(5)^{i}	0.92	2.14	2.875(4)	136
N(3)–H(3*B*)···O(3)^{ii}	0.92	2.06	2.932(8)	158
C(5)–H(5*C*)···O(l)^{iii}	0.98	2.34	3.313(4)	171
C(9)–H(9)···O(4)^{iv}	0.95	2.46	3.199(3)	134
II				
N(3)–H(3*B*)···O(8)^{ii}	0.92	2.08	2.958(7)	159
O(8)–H(8*A*)···O(9)^{i}	0.84	2.00	2.832(3)	170
O(8)–H(8*B*)···O(4)^{ii}	0.84	2.28	2.876(9)	128
O(8)–H(8*B*)···O(4)^{iii}	0.84	2.34	3.064(1)	145
O(9)–H(9*A*)···O(3)	0.84	2.07	2.820(3)	148
O(9)–H(9*B*)···O(1)^{v}	0.84	2.13	2.948(1)	164
C(10)–H(10)···O(6)^{vi}	0.95	2.42	3.254(3)	147

* Symmetry codes: ^{i} $-x, y-1, 3/2-z$; ^{ii} $-x, y, 3/2-z$; ^{iii} $x, 1-y, z-1/2$; ^{iv} $1/2-x, 3/2-y, 1-z$ (**I**); ^{i} $1-x, 1-y, 1-z$; ^{ii} $1-x, 2-y, 1-z$; ^{iii} $-x, 1-y, 1-z$; ^{iv} $x, y+1, z$; ^{v} $x+1, y, z$; ^{vi} $x-1, y-1, z-1$ (**II**).

dianion connect the adjacent metal centers through a bidentate chelating mode, leading to a one-dimensional (1D) linear chain running along the crystallographic *y* axis with the nearest Pb(II)···Pb(II) separation of 10.114 Å (Fig. 1b). The angle of three neighboring Pb^{2+} ions is 180°. Obviously, the NIP^{2-} anion in **I** adopts a *bis*-bidentate chelating binding fashion. Two polymeric chains of **I** are bound face-to-face by N–H···O hydrogen-bonding interactions between the amino group of AAP ligand and carboxylate moiety of NIP^{2-} anion (Table 3), yielding a double-chain architecture. Furthermore, these 1D chain pairs are periodically extended into a three-dimensional (3D) supramolecular network via weak C–H···O forces produced by methyl/phenyl substitute of AAP and ketonic/carboxylate moiety of AAP/NIP^{2-} ligand (Fig. 1c and Table 3).

Complex **II** with the formula of $\{[Pb(AAP)(NIP)] \cdot 2H_2O\}_n$ is a binuclear $\{Pb_2(AAP)_2\}$ subunit-based two-dimensional (2D) coplanar layer extended by bidentate chelating-bidentate chelating and bridging–NIP^{2-} anions. The asymmetric unit of **II** consists of one octa-coordinated Pb^{2+} ion, one fully deprotonated NIP^{2-} anion, one neutral AAP ligand with the firstly observed bidentate bridging binding mode, as well as two lattice water molecules. As illustrated in Fig. 2a, the holodirected Pb(II) site in **II** is completed by one N atom from the amino group of an AAP ligand and seven O donors, in which six are from four carboxylate groups of four NIP^{2-} anions and the last one belongs to the ketonic group of AAP molecule. The bond lengths of Pb–O and Pb–N are comparable to previous values [22–24]. It should be noted that the distance of $Pb-O_{carbonyl}$ is 2.832(3) Å, which is much longer (~0.2 Å) than that in **I** (Table 2).

Serving as an unusual ditopic connector, a pair of neutral AAP molecules adopt a rare bidentate N,O–bridging fashion, aggregating two holodirected Pb^{2+} ions into a binuclear $\{Pb_2(AAP)_2\}$ subunit with the intermetallic separation of 4.356(2) Å (Fig. 2b). Notably, the coordination mode of AAP ligand is different from each other despite the same donor atoms in **I** and **II**, in which the μ-N, O-AAP is firstly observed. Each dimeric $\{Pb_2\{AAP\}_2\}$ core in **II** is further extended by the NIP^{2-} dianion through a bidentate chelating-bidentate chelating and bridging coordination mode, generating a coplanar layer in the crystallographic *xy* plane. The closest Pb(II)···Pb(II) distance is 4.201(2) Å by bidentate chelating and bridging $-COO^{-}$, which is slightly shorter than that by μ-N, O-AAP. Additionally, one weak C–H···O hydrogen-bonding interaction is observed between aromatic ring

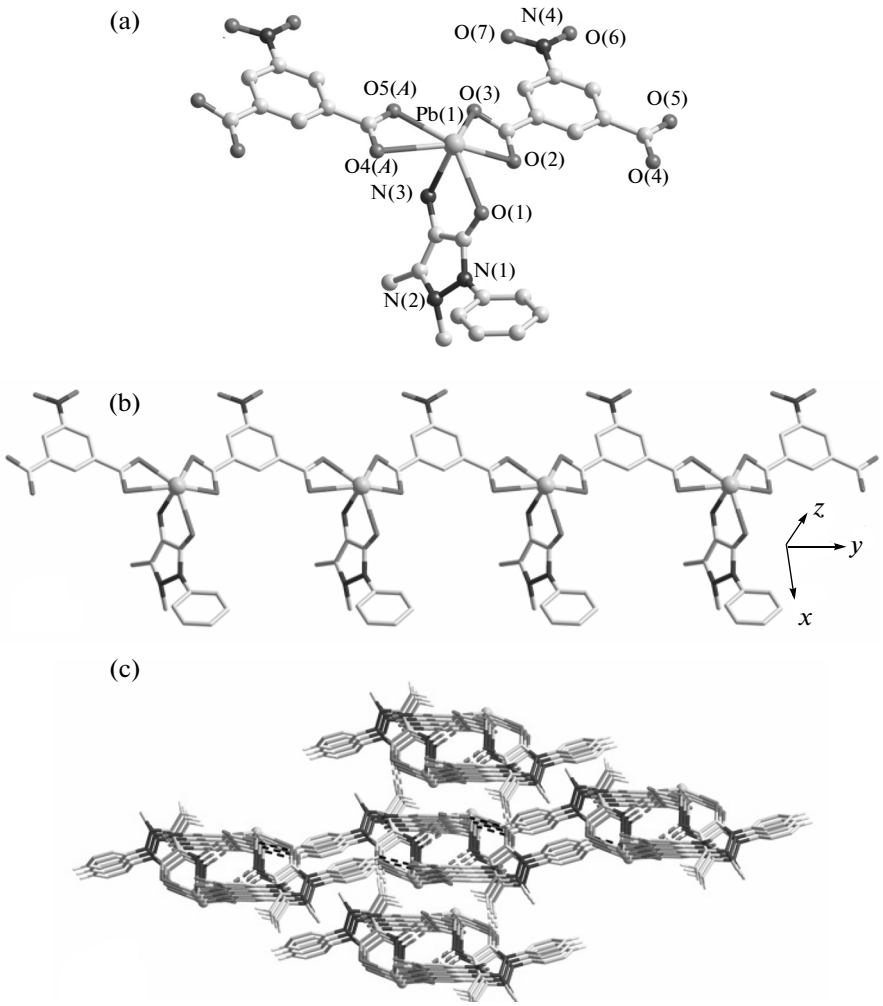

Fig. 1. Local coordination environments of Pb^{2+} ion in **I** (a) (H atoms were omitted for clarity, symmetry code: $A = x, y - 1, z$); 1D linear chain of **I** extended by NIP^{2-} anion (b); 3D supramolecular network of **I** formed by hydrogen-bonding interactions (c).

of AAP and nitro group of NIP ligand, which assembles the separate layers into a 3D network with two lattice water molecules entrapped in by non-covalent N–H···O and O–H···O interactions (Figs. 2c, 2d and Table 3).

Complex **I** could be thermally stable up to ~210°C and was followed by a consecutive weight-loss stage for the collapse of the polymeric chain (Fig. 3). The decomposition process of **I** was not completely finished until the highest temperature is up to 800°C. Instead, complex **II** exhibited a two-step weight-loss process. The first one began at room temperature and ended at 110°C, corresponding to the loss of two lattice water molecules (obsd. 5.5%, calcd. 5.6%). Then, a slow weight-loss process was observed, which was almost similar to that of **I**.

Luminescent behavior of **I**, **II** in the solid state were examined at room temperature to explore their potential applications as optical materials. As shown in Fig. 4, intense emissions located at 407 nm for **I** and 415 nm for **II** were obtained upon excitation the both samples at 300 nm. By contrast, free AAP and H2NIP molecules exhibited a broad emission centered at ~410 nm upon excitation at 300 nm under comparable conditions. Obviously, these two emissions of the complexes should be originated from intra– and/or interligand $\pi \rightarrow \pi^*$ transition and their slight red-shift may be resulting from the effect of metal-ligand coordination interactions.

In summary, two new MOFs assembled from the same reactant mixture, an extended linear chain for **I** and a dimeric $\{Pb_2(AAP)_2\}$-based coplanar layer for **II**, have been carefully isolated by pH-controlled evaporation method. The variable binding modes of the anionic NIP^{2-} and neutral AAP ligands are significantly dominated the overall structural difference.

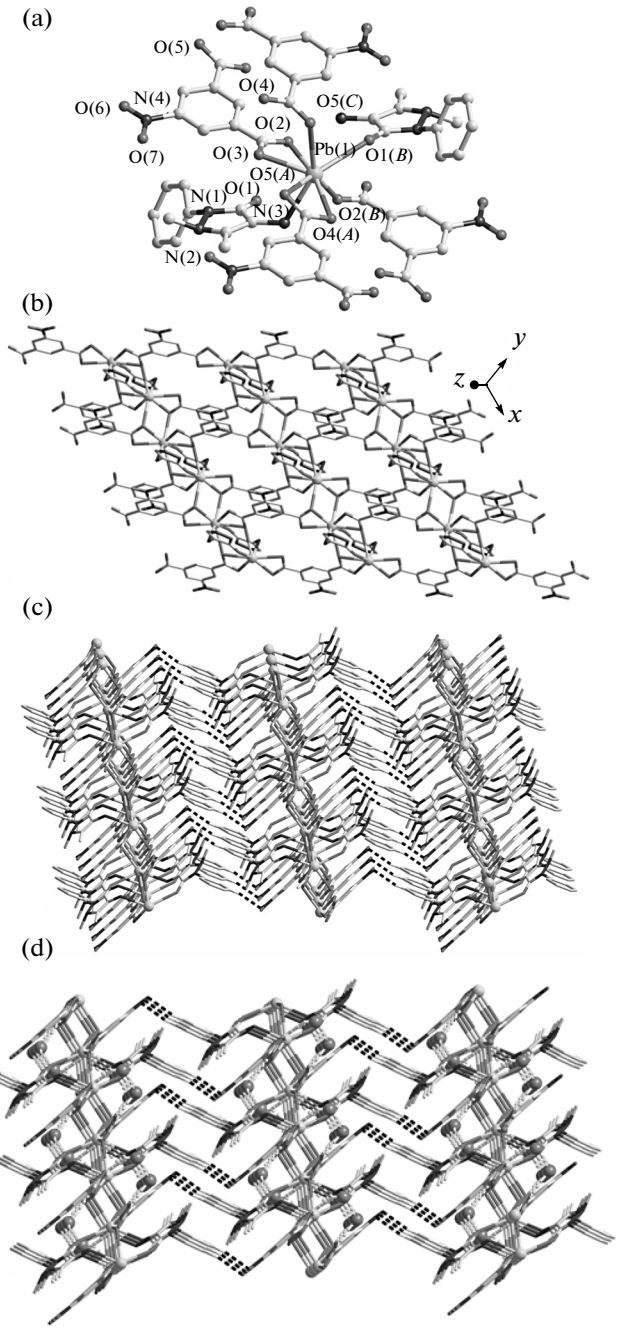

Fig. 2. Local coordination environments of Pb(II) atom in **II** (a) (H atoms were omitted for clarity, symmetry codes: $A = x + 1, y + 1, z$; $B = 1 - x, 1 - y, 1 - z$, $C = 1 - x, -y, 1 - z$); 2D layer of **II** (methyl and phenyl groups of AAP ligand were omitted for clarity) (b); 3D supramolecular network of **II** formed by C–H···O hydrogen-bonding interactions (c); 3D supramolecular network of **II** with lattice water molecules entrapped in (d).

Furthermore, both complexes display similar emissions originated from the intra– and/or inter-ligand electron transfer, suggesting their potential application as luminescent materials.

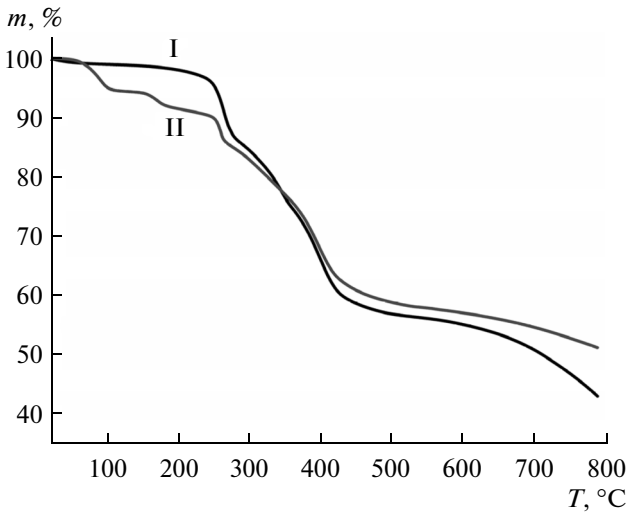

Fig. 3. TG curves for **I** and **II**.

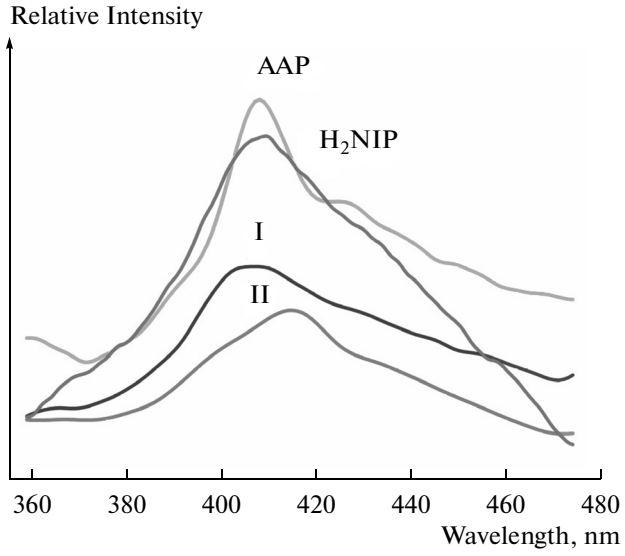

Fig. 4. Fluorescence spectra of **I**, **II** and free ligands in the solid state at room temperature.

ACKNOWLEDGMENTS

This present work was financially supported by the National Natural Science Foundation of China (grants 21171129, 21173157, 21371134, and 21303121), the Program for Innovative Research Team in University of Tianjin (TD12-5038), and Tianjin Municipal Education Commission (2012ZD02), which are gratefully acknowledged.

REFERENCES

1. Choi, H.J. and Suh, M.P., *J. Am. Chem. Soc.*, 2004, vol. 126, no. 48, p. 15844.
2. Uemura, K., Saito, K., Kitagawa, S., et al., *J. Am. Chem. Soc.*, 2006, vol. 128, no. 50, p. 16122.

3. Li, Y.W., Wang, L.F., He, K.H., et al., *Dalton Trans.*, 2011, vol. 40, no. 40, p. 10319.
4. Zhao, J.P., Han, S.D., Zhao, R., et al., *Inorg. Chem.*, 2013, vol. 52, no. 6, p. 2862.
5. Yang, E.C., Liu, Z.Y., Wang, X.G., et al., *CrystEngComm*, 2008, vol. 10, no. 9, p. 1140.
6. Yang, E.C., Liu, T.Y., Wang, Q., et al., *Inorg. Chem. Commun.*, 2011, vol. 14, no. 1, p. 285.
7. Mobin, S.M., Srivastava, A.K., Mathur, P., et al., *Inorg. Chem.*, 2009, vol. 48, no. 11, p. 4652.
8. Chen, L., Xu, G.J., Shao, K.Z., et al., *CrystEngComm*, 2010, vol. 12, no. 7, p. 2157.
9. Hu, T.L., Tao, Y., Chang, Z., et al., *Inorg. Chem.*, 2011, vol. 50, no. 21, p. 10994.
10. Bencini, A., Casarin, M., Forrer, D., et al., *Inorg. Chem.*, 2009, vol. 48, no. 9, p. 4044.
11. Zhao, J.P., Hu, B.W., Yang, Q., et al., *Inorg. Chem.*, 2009, vol. 48, no. 15, p. 7111.
12. Aijaz, A., Lama, P., and Bharadwaj, P.K., *Inorg. Chem.*, 2010, vol. 49, no. 13, p. 5883.
13. Roesky, H.W. and Andruh, M., *Coord. Chem. Rev.*, 2003, vol. 236, nos. 1–2, p. 91.
14. Wang, Q., Wu, M.J., Yang, E.C., et al., *J. Coord. Chem.,* 2008, vol. 61, no. 4, p. 595.
15. Hasani, M. and Rezaei, A., *Spectrochim. Acta, A*, 2006, vol. 65, no. 5, p. 1093.
16. Rosu, T., Pasculescu, S., Lazar, V., et al., *Molecules*, 2006, vol. 11, no. 11, p. 904.
17. Mahalingam, V., Chitrapriya, N., Fronczek, F.R., et al., *Polyhedron*, 2010, vol. 29, no. 18, p. 3363.
18. Hua, M.L., Morsalib, A., and Aboutorabi, L., *Coord. Chem. Rev.*, 2011, vol. 255, nos. 23–24, p. 2821.
19. Sheldrick, G.M., *SADABS, Program for Empirical Absorption Correction of Area Detector Data*, Göttingen (Germany): Univ. of Göttingen, 1996.
20. *SAINT, Software Reference Manual*, Madison (WI, USA): Bruker AXS, 1998.
21. Sheldrick, G.M., *SHELXTL, Structure Determination Software Programs*, Madison (WI, USA): Bruker Analytical X-Ray System, Inc., 2001.
22. Gabriel, C., Raptopoulou, C.P., Psycharis, V., et al., *Cryst. Growth Des.*, 2011, vol. 11, no. 2, p. 382.
23. Zhang, K.L., Liang, W., Chang, Y., et al., *Polyhedron*, 2009, vol. 28, no. 4, p. 647.
24. Foreman, M.R.St.J., Plater, M.J., and Skakle, J.M.S., *Dalton Trans.*, 2001, no. 12, p. 1897.